

In vitro and in vivo studies with recombinant clinical isolate-based respiratory syncytial virus in primary respiratory epithelial cultures, 2D airway organoids and small animal models

L. C. Rijsbergen¹, L. J. Rennick^{2,3}, M.M. Lamers¹, B. M. Laksono¹, A. D. Comvalius¹, P. R. W. A. van Run¹, R. W. Koutstaal¹, B.L. Haagmans¹, T. Kuiken¹, W. Paul Duprex², R. L. de Swart¹, R. D. de Vries¹
¹Department of Viroscience, Postgraduate School of Molecular Medicine, Erasmus MC, Rotterdam, The Netherlands ²Center for Vaccine Research, University of Pittsburgh, Pittsburgh, PA, USA

Introduction

Human respiratory syncytial virus (HRSV) usually causes mild respiratory tract infections, but a fraction of infants develops severe respiratory disease. From severe HRSV cases we learned that HRSV mainly infects ciliated epithelial cells in the airways. Subsequent inflammation and mucus production leads to plugging and occlusion of the small airways. In animal models, HRSV infection levels and inflammatory responses have predominantly been studied around the peak of infection. However, what happens at early time points remains largely unknown.

Our aim was to study the replication kinetics of HRSV-A and HRSV-B in vitro and to study the early viral spread of HRSV-A in vivo, because we hypothesize that this contributes to the risk of severe HRSV disease.

Methods



Conclusion

- (1) HRSV-A replicates faster than HRSV-B in cells from both the URT and LRT
- (2) HRSV infection in 2D AO cultured at ALI showed similar replication kinetics as in the bronchial cells
- (3) Clinical isolate-based rHRSV^{A11}EGFP(5) replicated to higher viral titres than laboratory-adapted rHRSV^{A2} in the URT of cotton rats and mice. Infection was predominantly present in ciliated epithelial cells in cotton rats and in the olfactory mucosa of mice.

In conclusion, using relevant in vitro and in vivo models we showed that HRSV replicates, already at early time points, in the entire respiratory tract. We also show that replication kinetics can vary significantly between strains and that HRSV tropism differs between mice and cotton rats.

Results

(1) Epithelial cells from all anatomical locations were susceptible to HRSV infection, although subgroup A viruses disseminated and replicated faster than the subgroup B virus. rHRSV infected mainly apical ciliated epithelial cells in all cultures, leading to cilia degeneration.

(2) HRSV replication kinetics and cytopathic effect in 2D AO cultures at ALI were comparable with the commercially available bronchial cultures: both rHRSV-A strains resulted in higher titers over time. Subgroup A viruses also had a replicative advantage in direct competition experiments.

(3) rHRSV^{A11}EGFP(5) replicated to higher viral titres than rHRSV^{A2}EGFP(5) in the upper respiratory tract of cotton rats and mice. Infection was mainly present in ciliated epithelial cells in cotton rats and in the olfactory mucosa of mice.

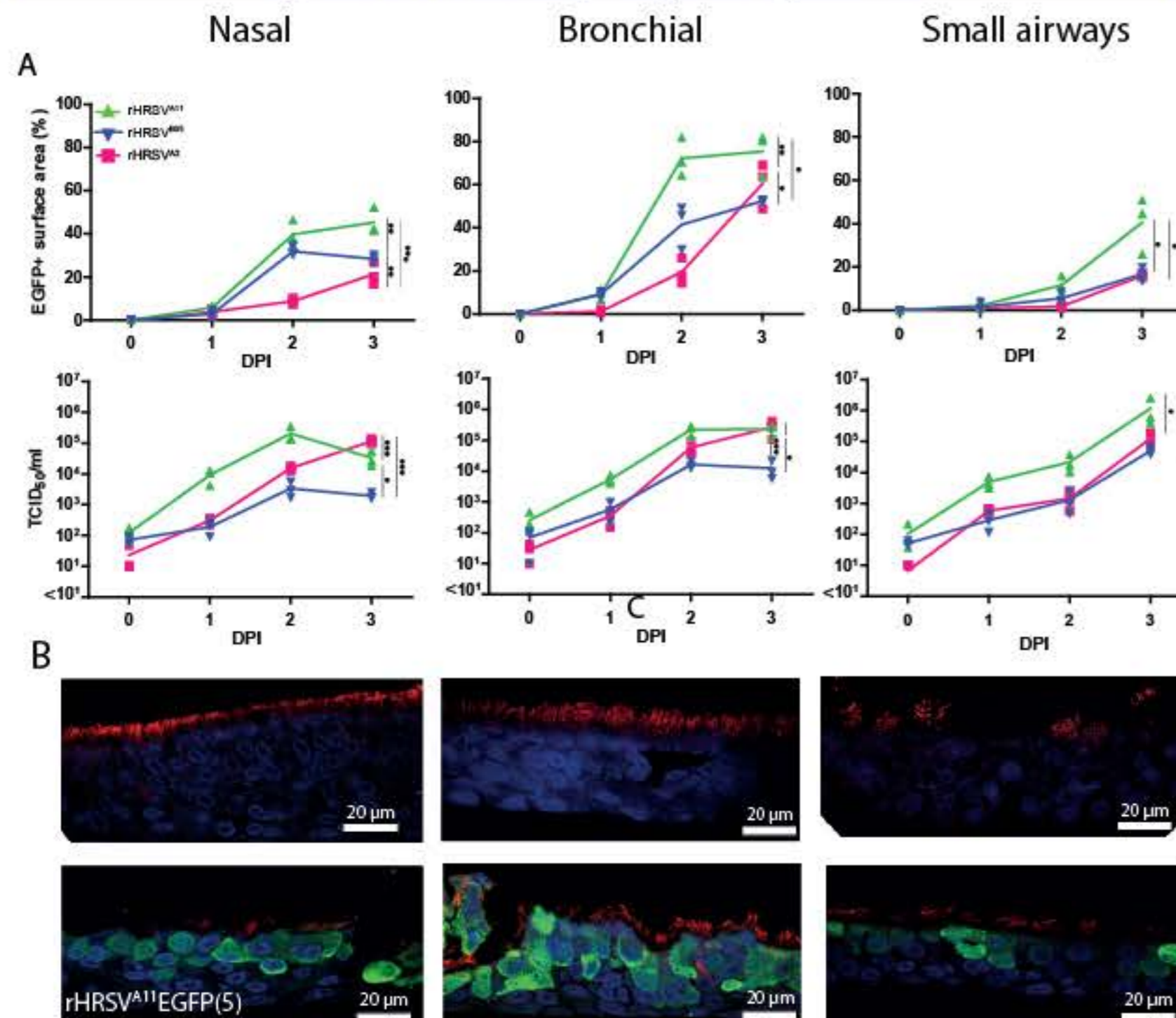


Figure 1. Replication kinetics and indirect immunofluorescence of rHRSV^{A2}EGFP(5), rHRSV^{A11}EGFP(5) and rHRSV^BEGFP(5) in nasal, bronchial and small airway cultures. (A) Nasal cells, bronchial cells and small airway cells were infected with rHRSV^{A2}EGFP(5), rHRSV^{A11}EGFP(5) or rHRSV^BEGFP(5) at a MOI of 0.5. The %EGFP+ surface area was determined by confocal laser scanning microscopy (CLSM) and the viral titers were determined by endpoint titrations of the apical supernatant (TCID₅₀/ml). One independent experiment performed in triplicate is shown. Differences between the growth curves were statistically analyzed by two-way ANOVA (*=0.05, **=0.01, ***=0.001, ****<0.0001). Mean and individual replicates are shown (B) Bronchial cells were infected with either rHRSV^{A2}EGFP(5), rHRSV^{A11}EGFP(5) or rHRSV^BEGFP(5) at a MOI of 0.5. Samples were fixed in formalin at 3 days post-infection (DPI) and embedded in paraffin. The paraffine-embedded slides were used indirect immunofluorescence (IIF) using antibodies against green fluorescent protein (HRSV, green), acetylated α -tubulin (cilia, red) and Hoechst (nuclei, blue) (Representative images are shown of rHRSV^{A11}EGFP(5).

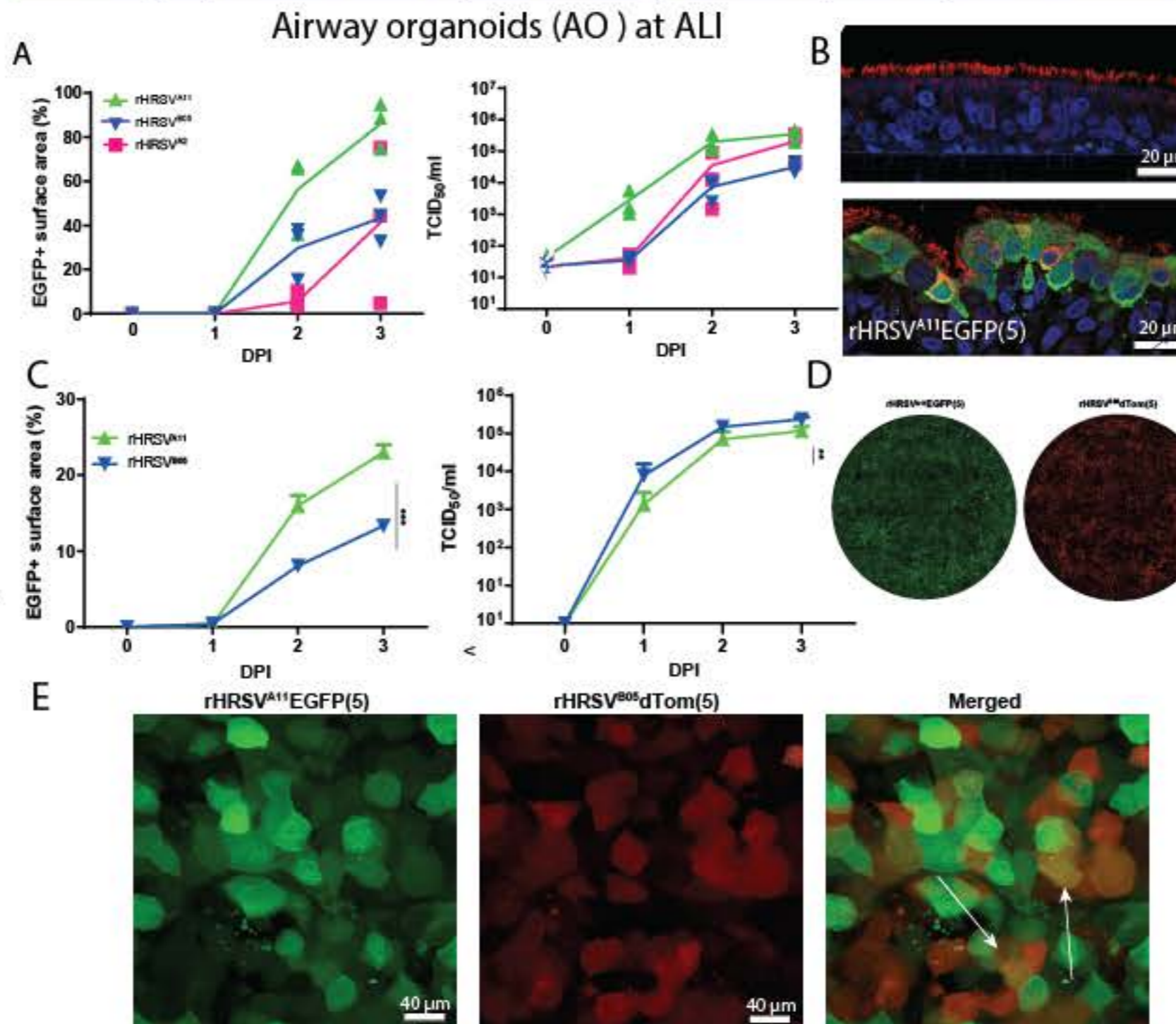


Figure 2. Replication kinetics and indirect immunofluorescence of rHRSV^{A2}EGFP(5), rHRSV^{A11}EGFP(5), rHRSV^BEGFP(5) and rHRSV^BdTom(5) in primary well-differentiated 2D AO cultures at ALI. (A) Primary well-differentiated 2D AO cultures at ALI were infected with rHRSV^{A2}EGFP(5), rHRSV^{A11}EGFP(5) or rHRSV^BEGFP(5) at a MOI of 0.5 (B) Samples were fixed in formalin at 3 DPI and embedded in paraffin. The paraffine-embedded slides were used for (IIF) using antibodies against green fluorescent protein (HRSV, green), acetylated α -tubulin (cilia, red) and Hoechst (nuclei, blue). Representative images are shown of rHRSV^{A11}EGFP(5). (C) 2D AO cultures at ALI were infected with rHRSV^{A11}EGFP(5) and rHRSV^BdTom(5) at equal MOI. The dissemination throughout the culture was imaged by CLSM (D) and transwell filters were analyzed at high resolution to identify double-infected cells (indicated by arrows) (E). The percentage EGFP+ surface area was determined by (CLSM) and the viral titers were determined by endpoint titrations of the apical supernatant (TCID₅₀/ml). Experiments were performed once in triplicate. Differences between the growth curves were statistically analyzed with a two-way ANOVA (*=0.05). Mean and individual replicates are shown.

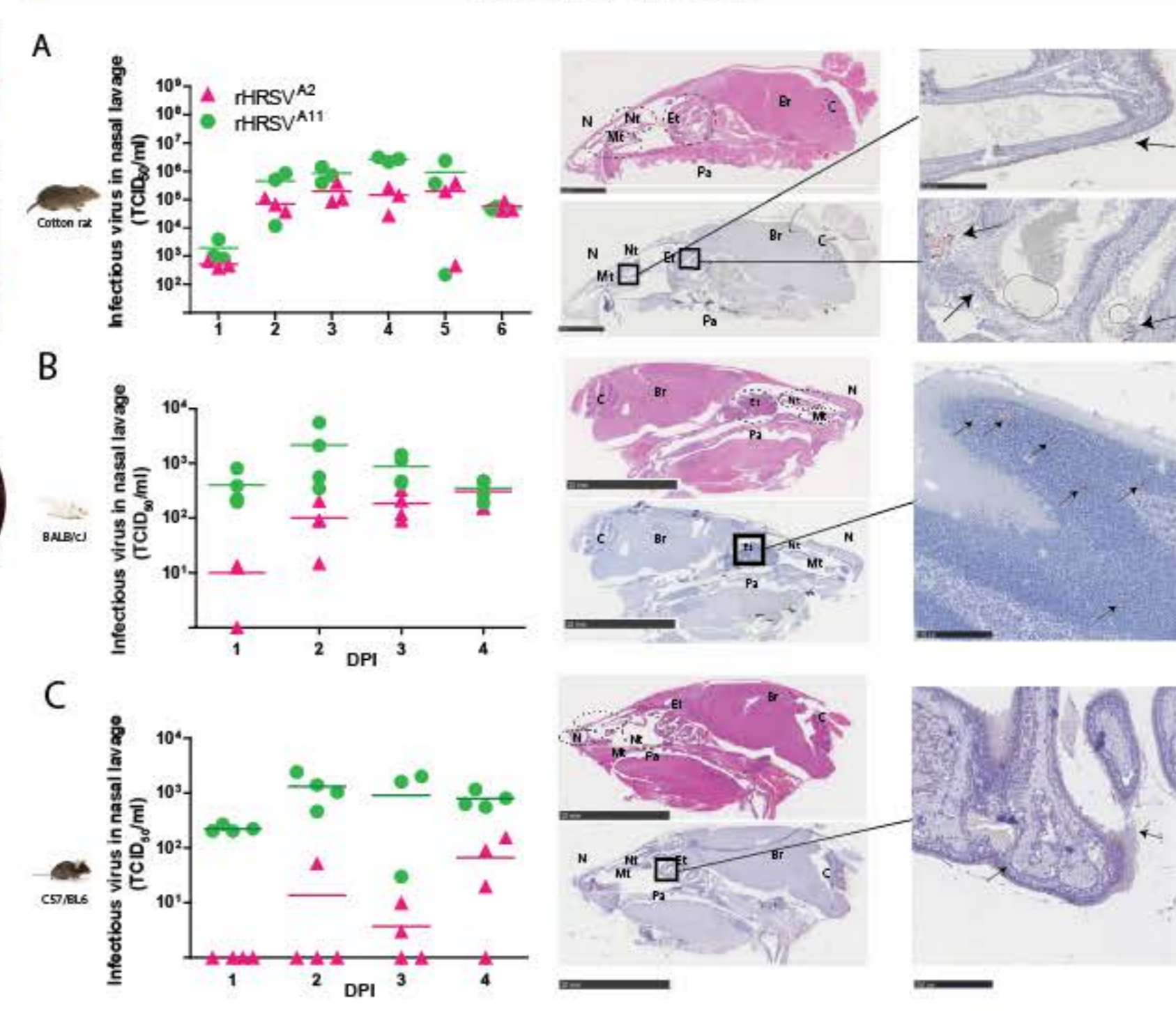


Figure 3. HRSV replication and tropism in the URT of cotton rats and mice. Viral loads in nasal lavages from cotton rats (A), BALB/cJ (B) and C57BL/6 mice (C). Inoculated intranasally with rHRSV^{A2}EGFP(5) or rHRSV^{A11}EGFP(5) and sacrificed at 1 – 6 or 1 – 4 days post-inoculation (DPI). Representative hematoxylin & eosin and immunohistochemistry images on formalin-fixed whole heads from cotton rats, BALB/cJ and C57BL/6 inoculated with rHRSV^{A11}EGFP(5) and sacrificed at 3 DPI. Arrows indicate EGFP+ cells. Indirect immunofluorescence staining on a formalin-fixed whole head of the cotton rat (E) BALB/cJ mouse (J) and the C57BL/6 mouse (O). N = nose, Mt = maxilloturbinate, Nt = nasoturbinate, Et = ethmoturbinate, Pa: palladium, Br: brain, C: cerebellum. Graphs depict means and standard deviations. The infectious virus (TCID₅₀/ml) of rHRSV^{A2}EGFP(5) were compared with those of rHRSV^{A11}EGFP(5) over time by using a polynomial regression model.